ORIGINAL ARTICLE

Pirfenidone reduces immune-suppressive capacity of cancer-associated fibroblasts through targeting CCL17 and TNF-beta

Hamidreza Aboulkheyr Es[1], Sareh Zhand[1], Jean Paul Thiery[2,3], and Majid Ebrahimi Warkiani[1,4,*]

[1]Faculty of Engineering and Information Technology, School of Biomedical Engineering, University of Technology Sydney, Sydney, New South Wales, Australia, [2]Department of Medical Oncology, Inserm Unit 981, Comprehensive Cancer Center, Institute Gustave Roussy, Villejuif, France, [3]Department of Regenerative Medicine and Health, Guangdong Laboratory, Guangzhou Regenerative Medicine and Health, Guangzhou, China, and [4]Institute of Molecular Medicine, Sechenov University, Moscow, Russia

*Corresponding author. E-mail: majid.warkiani@uts.edu.au

Abstract

Various factors in the tumor microenvironment (TME) regulate the expression of PD-L1 in carcinoma cells. The cancer-associated fibroblasts (CAFs) play a crucial role in regulating and rewiring TME to enhance their immune suppressive function and to favor the invasion of the malignant cells. Tumor progression may be retarded by targeting CAFs in the TME. Various studies highlighted the ability of targeting CAF with pirfenidone (PFD), leading to increased efficacy of chemotherapy. However, its potential for the reduction of immune-suppression capacity of CAFs remains to be elusive. Here, we assessed the effect of PFD on the expression of PD-L1 on CAF cells. Besides migration inhibitory effects of PFD on CAFs, the expression level of PD-L1 reduced in CAFs after treatment with PFD. The downstream analysis of released cytokines from CAFs showed that PFD significantly dropped the secretion of CCL17 and TNF-β, where a positive association between PFD-targeted proteins and PD-L1 was observed. These data suggest that the treatment of CAF within TME through the PFD may reduce the acquisition of CAF-mediated invasive and immune-suppressive capacity of breast carcinoma cells.

Key words: cancer-associated fibroblasts; pirfenidone; immune-suppression; PD-L1; microfluidic cancer model

> **INSIGHT BOX**
>
> The cancer-associated fibroblasts (CAFs) play a crucial role in regulating tumor microenvironment to enhance their immune-suppressive function. However, targeting this feature of CAFs remained to show. Herein, we employed an integrated *in silico* and experimental approach to investigate the therapeutic effects of pirfenidone on the immune-suppressive and cancer-promoting capacity of CAFs. The experiments utilize a 3D microfluidic *in vitro* model where tumor cells can be co-cultured with CAF cells. Employing this platform and our *in silico* data analysis, we show how pirfenidone inhibited the acquisition of CAF-mediated invasive and immune-suppressive capacity of breast carcinoma cells via suppression of CAFs activation and secretion of cancer-promoting cytokines. Our findings suggest that pirfenidone targeting CAFs may enhance the efficacy of the immune checkpoint inhibitors in breast carcinoma.

INTRODUCTION

Breast cancer (BC) is the most prevalent cancer in women and remains a significant cause of cancer-associated death, despite attempts to provide effective therapies. Patients diagnosed with TNBC do not benefit from endocrine or targeted therapies, and conventional chemotherapy is still considered the clinical state of the art for this subtype. Immune checkpoint blockade therapy has demonstrated success in various cancers but remains limited in TNBC treatment [1]. Among significant mechanisms responsible for tumour cells chemo/immunoresistance, there is increasing interest in understanding the role of the tumour microenvironment (TME) and its components in response to immune checkpoint inhibition [2–4]. Cancer-associated fibroblasts (CAFs) in the TME play a critical role in the complex process of tumour–stroma interaction. In aggressive BCs such as TNBC, the high abundance of CAFs associated with the aggressiveness of adenocarcinoma [5,6], disease recurrence [6–8], drug resistance [9,10] and lack of immune response [5,11]. Although tumour-promoting activities of CAFs are well explored [12], the immunomodulatory role of CAFs, as well as their potential application for therapeutic intervention, especially in the field of cancer immunotherapy, remains to be explored [13]. Thus, given their crucial role of CAFs in tumourigenesis and immunosuppression, in combination with the conventional treatments directed against carcinoma cells themselves, targeting CAFs might be a promising therapeutic approach. The recent approval of pirfenidone (PFD) for the treatment of idiopathic pulmonary fibrosis of lung relies on targeting activated fibroblast and their secretory functions [14].

Some recent studies were prompted to attempt co-targeting of CAFs and breast carcinoma cells with PFD and standard chemotherapy, respectively [15–17]. Although PFD was identified to mainly targets CAFs and their released cytokines, however, it remains elusive how PFD abrogate CAF-induced immune suppression. Herein, we hypothesized whether targeting CAFs with PFD would enhance tumour immunity for immunotherapy by inhibiting various factors such as PD-L1 and related cytokines.

MATERIAL AND METHODS

Figure 1 illustrates the workflow of this study, initiating from *in silico* data analysis of cancer genome alteration and gene-drug association of pirfenidone (Fig. 1A), followed by microfluidic-based co-culture of CAF cells and breast carcinoma cells in the device (Fig. 1B) and assessing the influence of pirfenidone on expression and the secretion of PD-L1 and associated cytokines (Fig. 1C).

In silico data analysis

The TCGA-BC genomic information and clinical data were downloaded from cBioportal data portal (https://www.cbioportal.org/) and analyzed under Bioconductor tools in R-Software (version 3.8). A detail description of used packages and related scripts to gene expression and mutation analysis is available at https://bioconductor.org/packages/release/bioc/vignettes/maftools/inst/doc/maftools.html. The protein–protein interaction and drug–protein interaction analyses were performed by using STRING PPI and SNITCH package under Cytoscape software (version 3.7.0).

Generation of CAF cells from normal fibroblasts

The normal fibroblasts (NFs) purchased from Lonza (Cat no: CC-2512) and maintained with FGM-2 Fibroblast Growth Medium-2 BulletKit (Cat no: CC-3132) according to provided protocol. To produce MDA-MB-231 conditioned medium, we cultured MDA-MB-231 (Cat no: HTB-26. ATCC) cells at 100% confluence with serum-free Dulbecco's Modified Eagle's Media (DMEM) supplemented with 100 U/ml penicillin and 100 μg/ml streptomycin
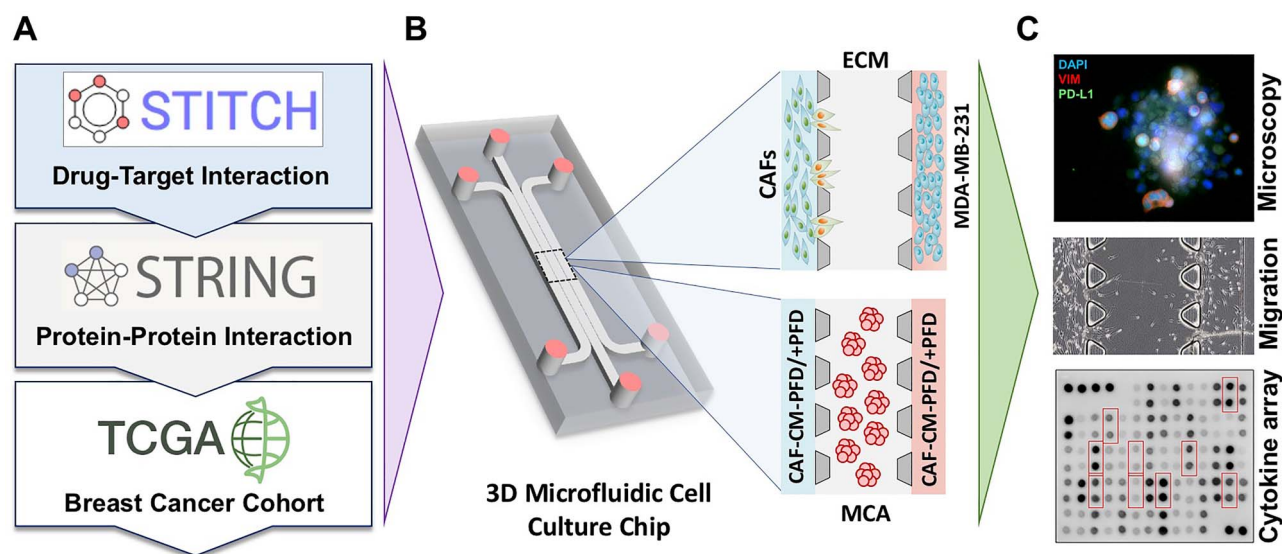
Figure 1. The workflow of study. (A) *In silico* data analysis of PFD through the drug–protein interaction, protein–protein interaction of PFD and its target proteins followed by genomic alteration analysis of these proteins across 1085 breast carcinoma samples deposited in The Cancer Genome Atlas (BRCA-TCGA). (B) The schematic design of used microfluidic cell culture device in this study for both co-culturing CAFs and breast carcinoma cells and culturing multicellular aggregates (MCAs) with CAF-CM included with or without PFD. (C) The downstream analysis performed on cells cultured in microfluidic device including immunofluorescent microscopy, distant migration analysis and cytokine profiling on derived conditioned medium from CAF cells.

(Sigma-Aldrich, St. Louis, MO, USA) for 48 hours. NFs were cultured at 80% confluence with condition medium derived from MDA-MB-231 for 48 hours.

Production of conditioned medium from CAF cells

We produced conditioned media of CAF (CAF-CM) using serum-free DMEM to exclude the effects of growth factors present in serum for the following experiments. The confluent (80%) CAF cells were maintained in serum-free DMEM for 48 hours. In experiments designed to analyze the effects of PFD on CAFs, 100% confluent CAFs were cultured in serum-free DMEM containing 100 μM PFD for 48 hours (CAF-CM + PFD) [18]. The conditioned media was centrifuged for 10 minutes at 1000 rpm after collection and stored at 80°C until use. The resulting conditioned media were used to stimulate BC cells. Proteins secreted into the supernatant were also examined through a cytokine profiling array against 42 targets.

Microfluidic device design and cell culture

The microfluidic tissue culture devices used in this study are purchased from AIM Biotech (Singapore). The devices consist of two media channels located on either side of an extended central region named gel channel (Fig. 1B). The 200-μl collagen gel solution (2.5 mg/ml) at pH 7.4 was prepared on ice by the mixture of 20-μl 10x PBS with 4-μl NaOH (0.5 N), 129.2-μl collagen type I (Corning), 10-μl freshly trypsinized and dissociated MCF7 at 6×10^5 cells/ml (for 2D studies) or 10-μl cell suspension medium with 50–100 tumor spheroids (for 3D studies), and 22.9-μl deionized water. The collagen gel solution containing the MCF7 aggregates or single cells was then loaded into the central gel region of the device and kept in the cell culture incubator at 37°C and 5% CO_2 for 40 minutes to allow gel polymerization via thermal cross-linking. Devices with gel only (no embedded cells, control) were prepared as described above except adding cell suspension. Immediately after gel polymerization, DMEM or CAF-CM media was subsequently introduced to respective media channels. In case of migration assay, the central channel was filled with prepared collagen gel solution, while the side channels were loaded with 2000 cell/120-μl cultured medium.

Culturing single cells and multicellular aggregate in the microfluidic device

In order to obtain cell aggregates with the appropriate size for 3D studies, MCF7 cells were trypsinized and resuspended as individual cells at 100 000 cells/ml in DMEM and cultured for 3 consecutive days onto a 100-mm ultra-low attachment dish (Corning Inc, NY, USA). Aggregates were collected and filtered in two consecutive filtration steps: (i) 40-μm filtration, in order to exclude cell aggregates smaller than 40 μm, and (ii) 100-μm filtration, in order to exclude aggregates larger than 100 μm in diameter, and centrifuged by $250 \times g$ for 5 minutes to separate them from the supernatant. For 2D studies, cells were harvested with Trypsin/EDTA and centrifuged at $200 \times g$ for 5 minutes. Cells were resuspended in growth medium and mixed with collagen type I solution for a final concentration of 6×10^5 cells/ml total collagen solution as described above.

Immunofluorescent staining

Cell culture media was removed from the devices, and samples in the microfluidic devices were first rinsed in $1 \times$ PBS through the adding 70 μl of PBS into one port and another 50 μl into the opposite connected port of a media channel. Then, the cells fixed with 4% paraformaldehyde (Sigma-Aldrich, St. Louis, MO, USA) for 15 minutes at room temperature. Next, 0.1% Triton-X 100 (Sigma-Aldrich, St. Louis, MO, USA) was added, and the device was incubated for 10 minutes before blocking by BSA 1% (cat no: A5611. Sigma-Aldrich, St. Louis, MO, USA) for 2 hours, followed by staining of cells for α-SMA (1:100, cat no: ab197240. Abcam), Vimentin (1:200, cat no: 677804. Biolegend) and PD-L1(1:200, cat no: ab214958. Abcam). The mean fluorescent intensity (MFI) of images was analyzed using Cell-Sense software (Olympus, Japan). The NFs and cancer cells cultured in DMEM are considered as control. To cell morphogenesis analysis, the cell area, circularity and aspect ratio were analyzed using MorphoLibJ in ImageJ software.

Cytokine array

The cytokine profiling of CAF-conditioned media included with and without PFD analyzed against a panel of 42 different inflammatory and cancer-promoting cytokines using the Human Cytokine Antibody Array (cat no: ab133997. Abcam) according to the manufacturer's instructions.

Statistical analysis

All experiments were performed in three independent technical replicates ($n = 3$). The results of quantitative experiments were expressed as mean ± SD. Statistical analysis was performed with Student t-test. *P-value <0.05 was considered as a statistically significant and ****P-value <0.005 was considered as an extremely significant. Microscopic images are representative images from three independent experiments. The MFI was measured and analyzed using ImageJ software.

RESULTS

Association between CAF derived cytokines with PD-L1

According to the drug-bank information, PFD is an orally active small molecule that may inhibit collagen synthesis, down-regulate production of multiple cytokines, and block fibroblast proliferation and stimulation in response to cytokines. In an *in silico* analysis, first, we analyzed the drug–protein interaction of PFD (Fig. 2A). As depicted in Fig. 2A, PFD potentially targets IL-10 (score: 0.836), TGFB1 (score: 0.859), TIPM1 (score: 0.824) and FN1 (score: 0.822) (Fig. 2A). Interestingly, the tissue-specific protein–protein interaction analysis between proteins targets of PFD and immune suppression protein PD-L1 (CD274) showed a positive correlation between IL10, and IL6 with CD274 (PD-L1), IL8 (CXCL8) and TNF-β (LTA) in BC (Fig. 2B). Following these observations, we analyzed alteration frequencies of these proteins across 1085 breast carcinoma samples deposited in TCGA (Fig. 2C). As shown in Fig. 2C, high expression of TNF-β, TGF-β1, IL8, IL6 and IL10 was identified across patients diagnosed with breast invasive ductal carcinoma (IDC) compared with other subtypes such as breast invasive lobular carcinoma and mixed ductal-lobular carcinoma (Fig. 2C). In line with the PPI interaction results, the Pearson correlation analysis shows a positive correlation between IL6, IL8, IL10 and TNF-β with PD-L1 among samples with IDC subtypes (Supplementary Fig. 1). It is well established that tumor stromal cells, particularly CAFs, can reprogram cancer cells in TME through the secretion of various cytokines and induce an immune-suppression TME [19]. In line with these findings, we
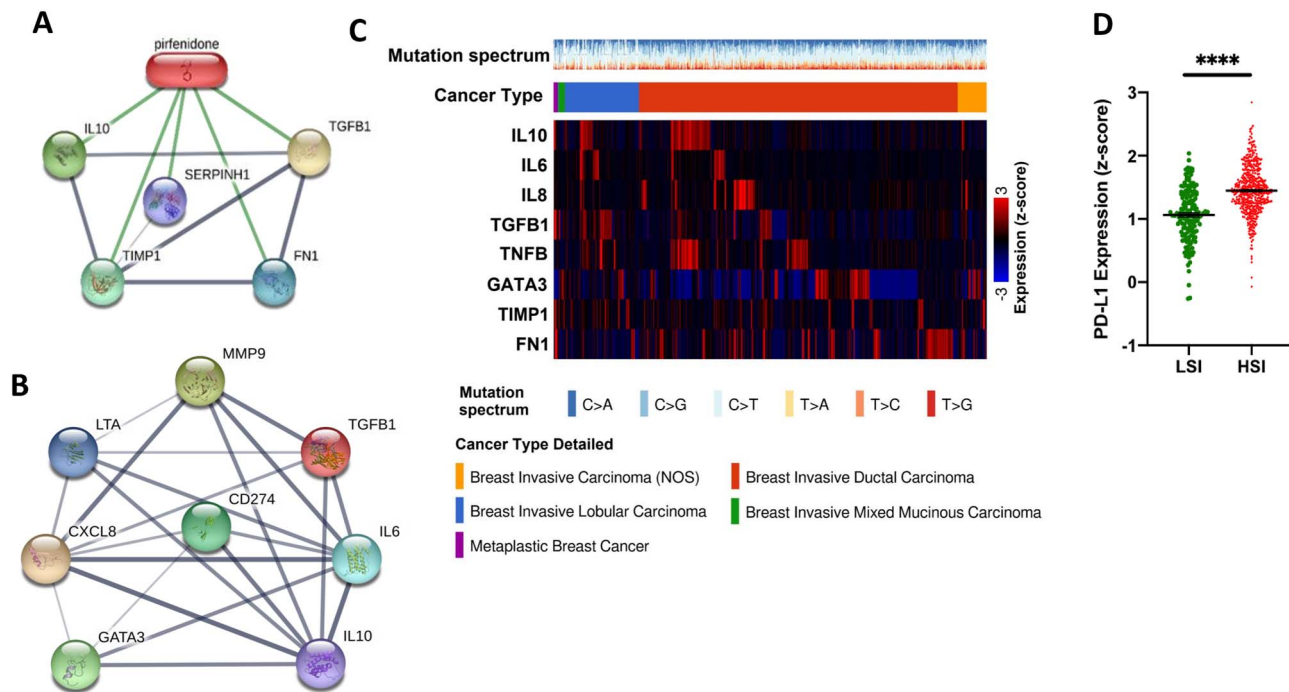
Figure 2. *In silico* analysis of PFD target proteins and their alterations across breast carcinoma samples in TCGA. (A) Drug–protein interaction analysis results showing main targets of PFD. (B) The protein–protein interaction results retrieved from STRING database. The result shows a positive correlation between PFD protein targets with various interleukins including IL6 and IL8 (CXCL8), TNF-β (LTA) and PD-L1 (CD274). (C) The oncoprint results of genomic alteration status of PFD targets proteins and their positive associated proteins across 1085 breast carcinoma samples in TCGA. The data depict a high expression level of TNF-β, IL8 and IL10 in patient with IDC sub-types in comparison with other subtypes. (D) Comparison between the expression level of PD-L1 among samples with high and low stromal index (P < 0.005).

analyzed the expression of PD-L1 among samples with low- and high-stromal index (LSI/HSI) according to their ESTIMATE score (Fig. 2D) [20]. As we expected, a significant expression of the PD-L1 (Fig. 2D) was observed among the HSI tumor samples compared with the LSI group, indicating a positive association between the proportion of tumor stromal cells and the expression of PD-L1. Taken together, these data suggest that targeting CAFs and its released cytokines may reduce the immune-suppression capacity of TME through the reduction of PD-L1 expression.

CAFs induce a phenotype switch in cancer cells

To generate CAF cells, we cultured normal human lung fibroblasts with condition medium derived from MDA-MB-231 for 72 hours (Fig. 3A), followed by the characterization of induced cells in terms of expression of the CAF marker alpha-smooth muscle actin (α-SMA) and also the expression of PD-L1. As an expression of α-SMA is one of the hallmarks of CAF cells, we observed a significant expression of α-SMA in cultured fibroblasts with MDA-MB-231 condition medium compared with the cells cultured with DMEM (Fig. 3B and C). Various studies have shown the expression of PD-L1 on CAF cells [5]. In line with these results, we assessed the expression of PD-L1 on generated CAFs at the protein level. As depicted in Fig. 3D, our generated CAFs significantly expressed PD-L1 compared with the NFs.

Numerous *in vitro* and *in vivo* studies highlighted the migration and recruitment of CAF cells to the TME [21]. To model this characteristic feature of CAFs, we performed a co-cultured assay in a three channels 3D microfluidic cell culture device (Fig. 4A), where the central channel was filled with collagen type-I, while CAF cells and cancer cells were cultured in one of the

two side channels (Fig. 4A). Compared with the NFs, the CAFs not only invaded the central channel containing collagen type-1 and migrated toward the cancer cell containing channel (Fig. 4B) but also significantly expressed both α-SMA (Fig. 4C) and PD-L1 (Fig. 4D), indicating a *trans*-differentiation of NFs into CAF.

The phenotypic transformation from an epithelial- to mesenchymal-like is a significant step in invasion and metastasis of carcinoma cells, which can be induced through the tumor stromal cells, particularly CAF cells. To assess the effects of cytokines derived from CAFs on the phenotypic switch of carcinoma cells, we cultured MCF7 cells known as an epithelial-like breast carcinoma with CAF-CM for 72 hours, followed by a shape descriptor analysis. As depicted in Fig. 5, in line with a microscopic observation (Fig. 5A), increase in aspect ratio and reduction of circularity level indicated phenotypic switch of carcinoma cells from epithelial to a mesenchymal-like phenotype acquiring invasive phenotype induced by CAF-CM (Fig. 5B and C. P < 0.001). These results are in line with previous observations showing that CAF cells directly or indirectly able to reprogram cancer cells toward the induction of an aggressive TME.

CAFs-induced expression of PD-L1 on PD-L1 low cancer cells

To determine whether CAFs cells able to induce the expression of PD-L1 on BC cells, we generated tumor aggregate from MCF7 cells, a PD-L1 negative BC cell [22] and cultured with CAF condition medium (CAF-CM) in a microfluidic device for 72 hours (Fig. 6A). The generated aggregates mixed with collagen type I as standard ECM and were loaded in the central channel of the device followed by filling the side channels with standard cell
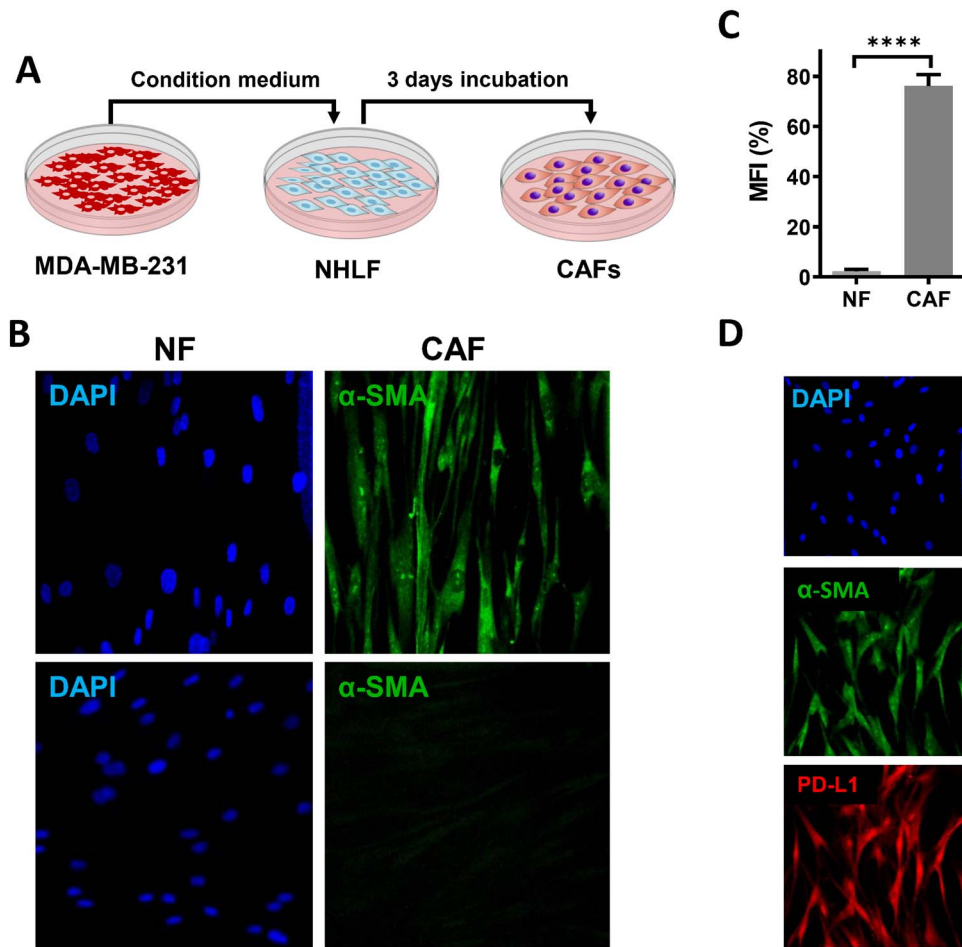
Figure 3. Transformation of NF to CAFs and its characterization. (A) Schematic of method used to generate CAF from NFs. (B and C) Confocal immunofluorescence image of α-SMA expression (green) in generated CAFs compared with the NF. The nucleus is stained with DAPI (blue) (scale bar: 20 µm. $P < 0.005$). (D) Expression of PD-L1 in CAFs (scale bar: 50 µm).

culture medium (control) or CAF-CM (Fig. 6A). Interestingly, CAF-CM significantly increased the expression of both PD-L1 and VIM at the protein level in MCF7 aggregates (Fig. 6B–D). Notably, we observed low expression of PD-L1 and VIM in the control group. We previously reported [22] the effects of ECM and tumor cell aggregation on the expression of PD-L1 and VIM; here, we show that CAF-CM also induced the expression of these genes. These data suggest that cytokines released from CAF cells play an immune suppression role through the induction of PD-L1 expression.

Pirfenidone reduces invasion and migration capacity of CAF and cancer cells

To assess the inhibitory effects of PFD on invasion and migration capacity of both BC cells and CAFs, first, we cultured CAF cells at the highest confluence in a serum-free medium with PFD (100 µM) for 48 hours (CAF-CM/+PFD), followed by culturing MCF7 cells with this generated condition medium.

MCF7 cells cultured with CAF-CM + PFD showed a significant increase in circularity level and a slight reduction in aspect ratio and cell area (Fig. 7A–D) as compared with untreated conditioned medium (Fig. 7A middle), indicating that treating CAFs with PFD may inhibit invasive properties of cancer cells induced by CAFs. To show migratory inhibition effects of PFD,

we performed co-culture assay of CAFs and invasive BC cell line MDA-MB-231 in the presence (+PFD) or absence (−PFD) of PFD (100 µM) in a 3D cell culture microfluidic device for 72 hours (Figs 4A and 7E). Figure 7E shows a snapshot image of the migration of cells through the collagen type-1 toward the opposite channel in three different time-points. We found that PFD reduced the migration of the cells in a time-dependent manner, where after 48 hours, a significant reduction in migration distance of both cells was observed. The maximum inhibition recorded after 72 hours of treating cells with PFD (Fig. 7E and F).

Pirfenidone reduces expression of PD-L1 on CAF cells by targeting various cytokines

Next, we assessed the expression level of PD-L1 protein on CAF cells treated with PFD. Interestingly, we observed that in comparison with non-treatment samples, PFD treatment not only reduced the level of s-SMA in CAFs but also significantly decreased the level of PD-L1 at protein level (Fig. 8A and B). To better understand the PFD effects, we assess the expression and secretion of various cytokines in both treated- and non-PFD treated groups (Fig. 9). We found that PFD significantly dropped the secretion of TNF-beta and CCL17 in CAF cells in comparison with the non-treated group (CAF-CM-PFD) (Fig. 9A, B and E).
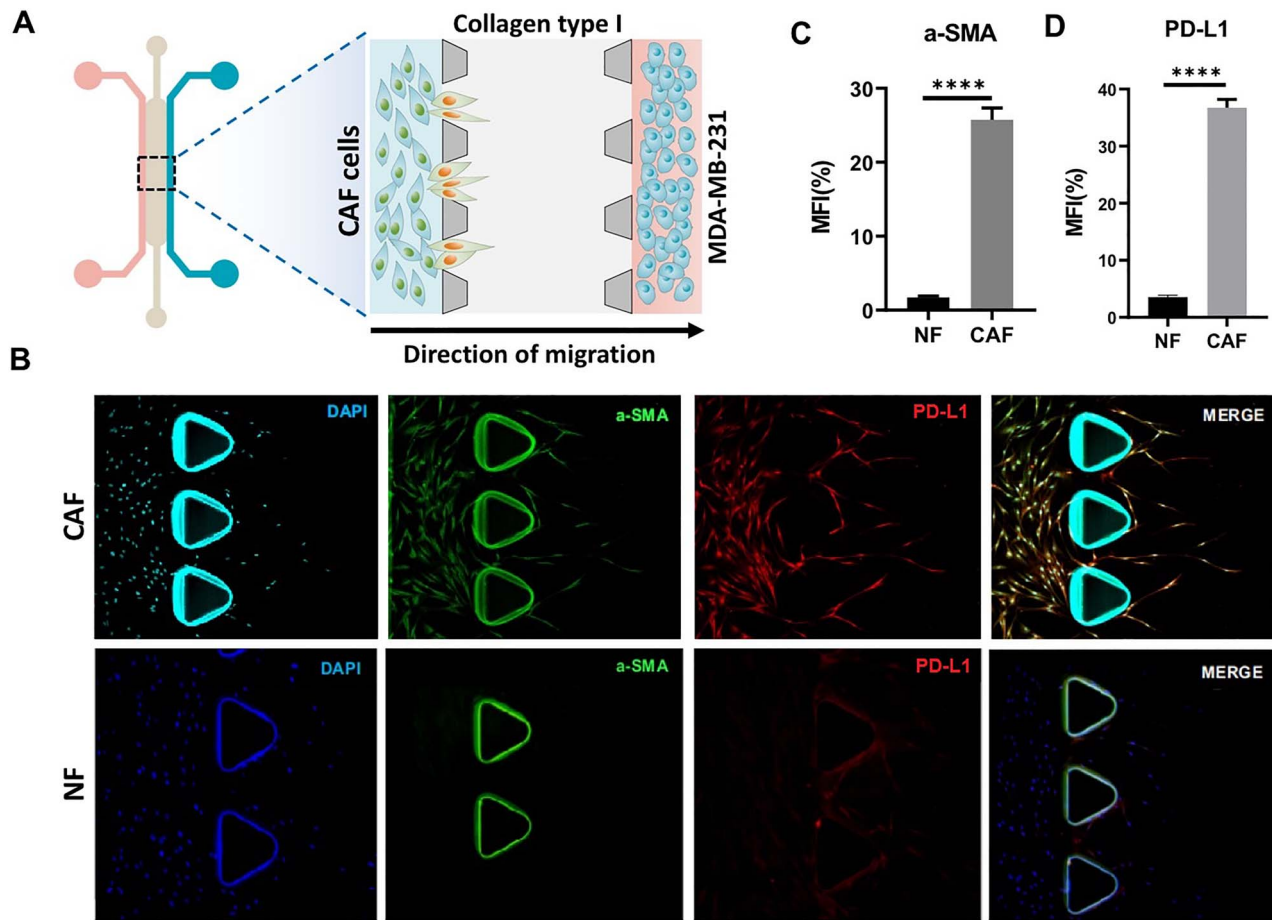
Figure 4. Migration of CAFs. (A) The schematic design of experiments in a microfluidic device by culturing CAFs in one of side channels, while the MDA-MB-231 cells are cultured in opposite channel. The central channel is filled by collagen type-I as a standard ECM. (B) Immunofluorescence image of migrating CAFs toward opposite channel where invasive BC cells are seeded. The CAFs highly expressed both α-SMA (green) and PD-L1 (red) in comparison with NF (scale bar: 100 μm). (C and D) Quantitative analysis of MFI of α-SMA and PD-L1 expression in CAFs and NF ($n = 3$) ($P < 0.005$).

Besides, the level of other cytokines, including OSM, CSF, IL6, IL8 and CXCl1, was reduced following treatment with PFD. Additionally, the PPI network analysis showed a positive association between PFD targeted cytokines and PD-L1, particularly IL6, CCL17 and CXCL1 (Fig 9I). Taken together, these data suggest that PFD can reduce both invasion and immune suppression capacity of cancer cells in TME by targeting various cytokines in CAF cells.

DISCUSSION

Within the tumor-stromal milieu, CAFs are the most prominent cell type and are known to be critical contributors to tumor progression, metastasis and drug resistance against a broad spectrum of therapies including immunotherapy [2]. CAF directed therapy designed to either eliminate them or potentially reprogram them back to their normal resting phenotype is showing some promise. For example, a recent study on pancreatic adenocarcinoma has demonstrated that targeting vitamin-D receptor by calcipotriol in stromal cells can reprogram pancreatic cell-derived CAFs, resulting in higher intra-tumoural penetration of gemcitabine, tumor shrinkage and improved patient survival [23]. Although numerous studies highlighted various therapeutic agents to target CAFs in different cancers [15, 16, 24, 25], its effects on the reduction of immune suppression potential of CAFs in breast carcinoma remained to show [26]. Herein,

for the first time, we show that targeting CAFs with PFD can retard the immunosuppressive capacity of CAFs and, consequently, its PD-L1 expression stimulation on breast carcinoma cells through production blockage of various cytokines including CCL17, CXCL1, TNF-β, IL6 and IL8 in CAFs. Additionally, through the using microfluidic co-culture platform [27–29], we demonstrated that the treatment of CAF cells with PFD not only reduces the expression of a-SMA in CAF cells but also decreases the migration potential of CAFs and breast carcinoma cells in a time-dependent manner.

A large number of studies highlighted the critical role of these factors in the interaction of the tumor–stromal cell toward the induction of an immune-suppressive TME [5]. Studies on genome and proteome analysis of CAFs showed that CAFs exhibit particular immunomodulatory secretome including but not limited to these factors to reshape TME toward tumor progression and potentially regulate the innate immune suppression in several ways [30–34]. The CCL17 was reported as a key element in the re-education of monocytes and the generation of tumor-associated macrophages that expressed IDO and PD-L1 [35]. Additionally, it has been shown the production and secretion of CCL17 within TME through the CAFs trigger recruitment of Myeloid-derived suppressor cells and T_{reg} cells to TME promoting an immunosuppressive TME in various cancers [36–39]. Furthermore, Omland and colleagues
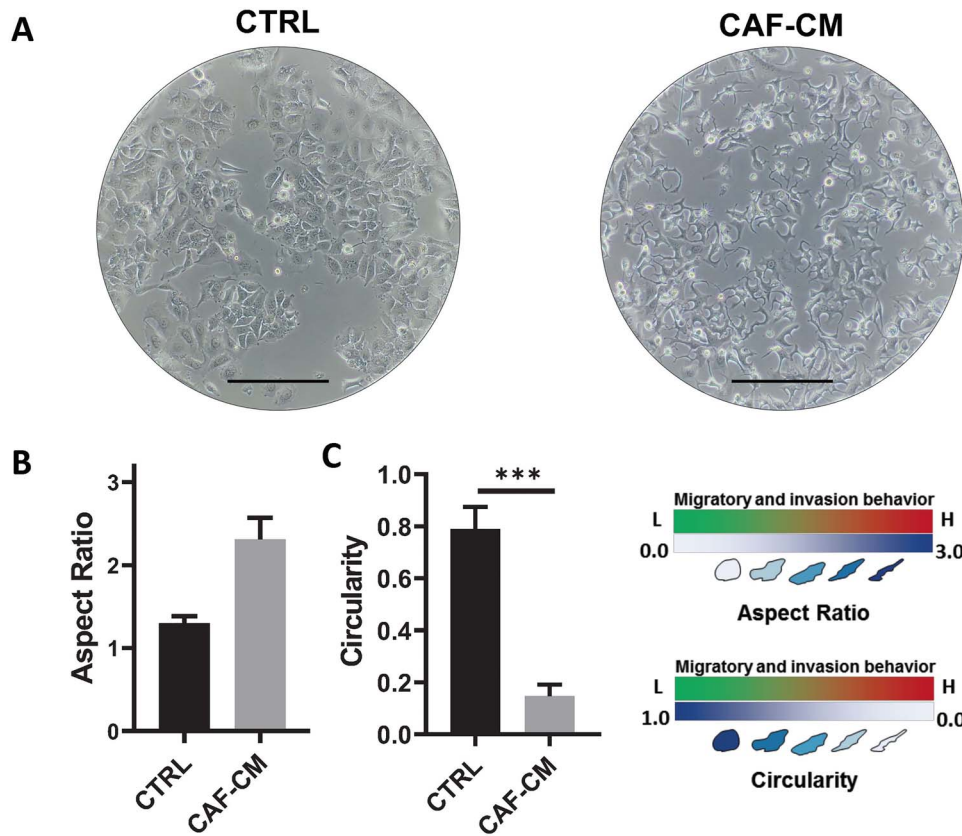
Figure 5. Phenotypic transformation of MCF7 cells cultured with CAF-CM. (A) Microscopic image of MCF7 cells cultured with CAF-CM (right) and conventional culture medium (left), showing a phenotype switch in group of cells cultured in CAF-CM toward an invasive behavior compared with the control group. (B and C) The quantitative results of morphometric analysis of aspect ratio (B) and circularity level (C) in transformed cells ($n = 3$).
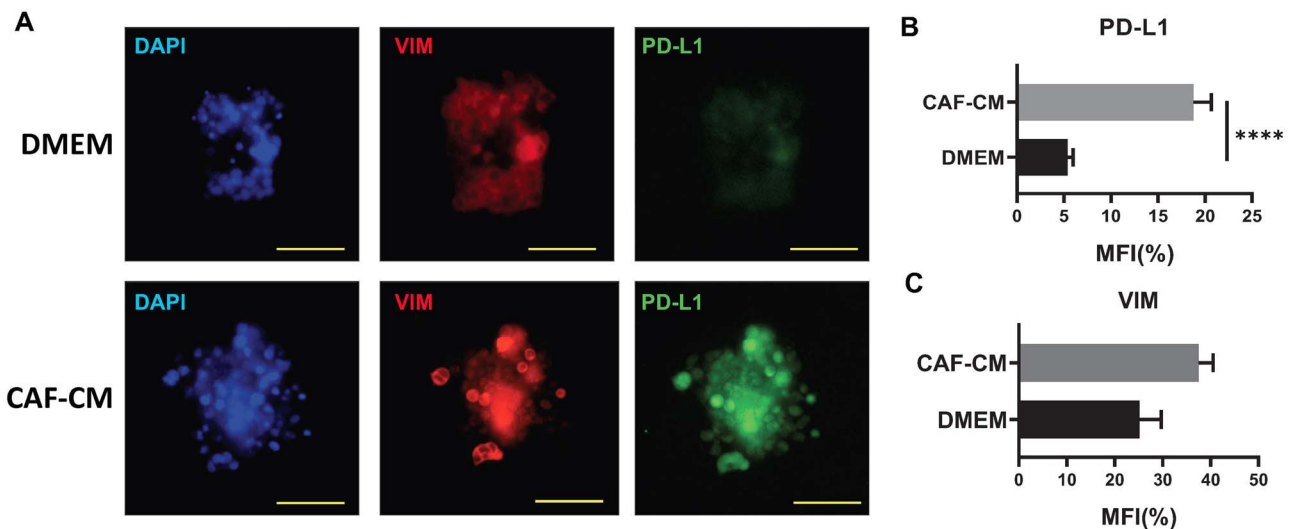

Figure 6. Culturing MCF7-derived MCA with CAF-CM. (A) Immunofluorescent image of MCA cultured with either CAF-CM or conventional culture medium (DMEM) and expression of VIM (red), PD-L1 (green) and nucleus (blue) in these group of cells (scale bar: 100 μm). (B and C) Quantitative analysis of MFI of PD-L1 (B) and VIM (C) in MCAs. CAF-CM significantly induced expression of PD-L1 ($n = 3$) ($P < 0.005$).

[40] reported that CXCL12 and CCL17 that secreted from resident CAFs within Cutaneous basal cell carcinoma TME increase tumor progression and immunosuppression.

The immune-modulation role of inflammatory cytokines has been evident extensively.

A large amount of *in vitro* and *in vivo* studies documented that the secretion of IL-6 and IL-8 by CAFs positively regulates the expression of PD-1/PD-L1 axis in TME, in which targeting these interleukins may reverse immune resistance [34,41–43]. In this regard, Tsukamoto and colleagues [41] found that combinatorial
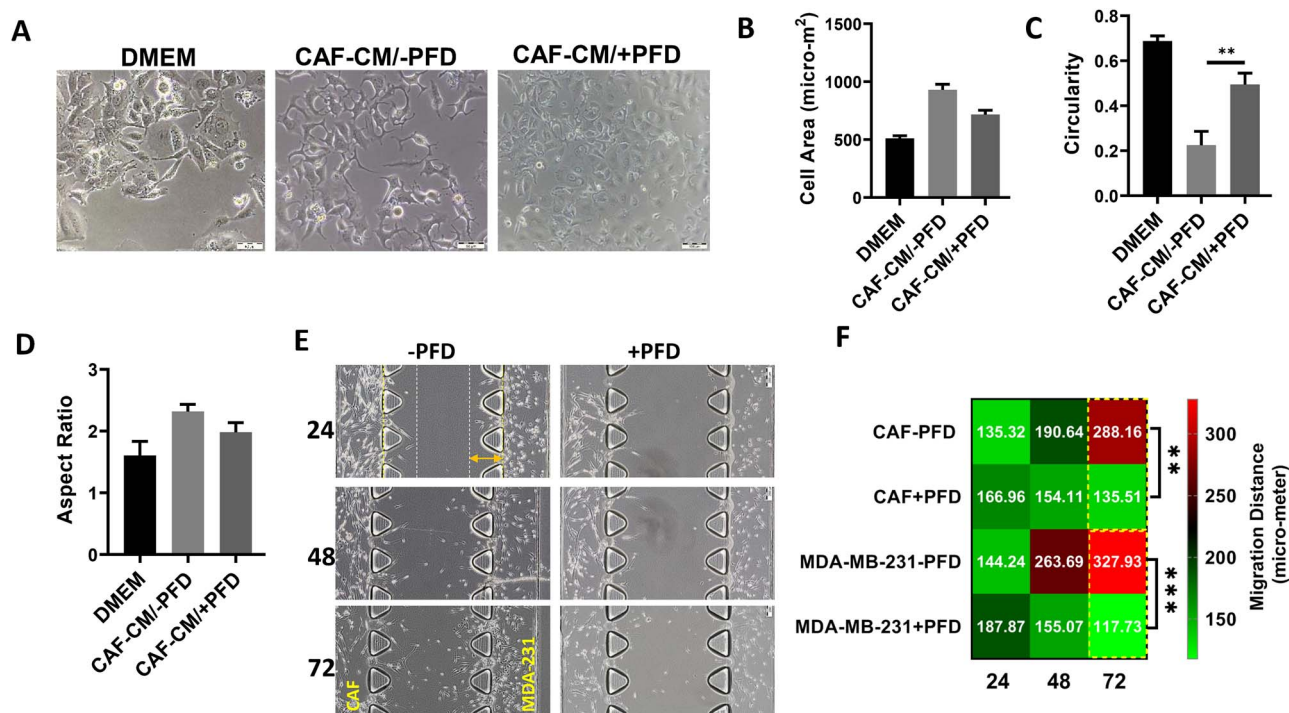
Figure 7. Effects of PFD on phenotype transformation and migration of cells. (A) Representative image of cells cultured with CAF-CM included with and without PFD for 72 hours. (B–D) Quantitative analysis of morphometric parameters: cell area (B), circularity level (C) and aspect ratio (D) of cells cultured in conventional DMEM and CAF-CM including with or without PFD. (E) A snapshot of co-culture microfluidic device contained CAF cells and breast carcinoma cells cultured with serum-free medium included with or without PFD. The central channel is filled with collagen type-I as ECM (scale bar: 200 μm). (F) Quantitative analysis of migration distance (μm) of both CAF cells and breast carcinoma cells cultured in microfluidic device.
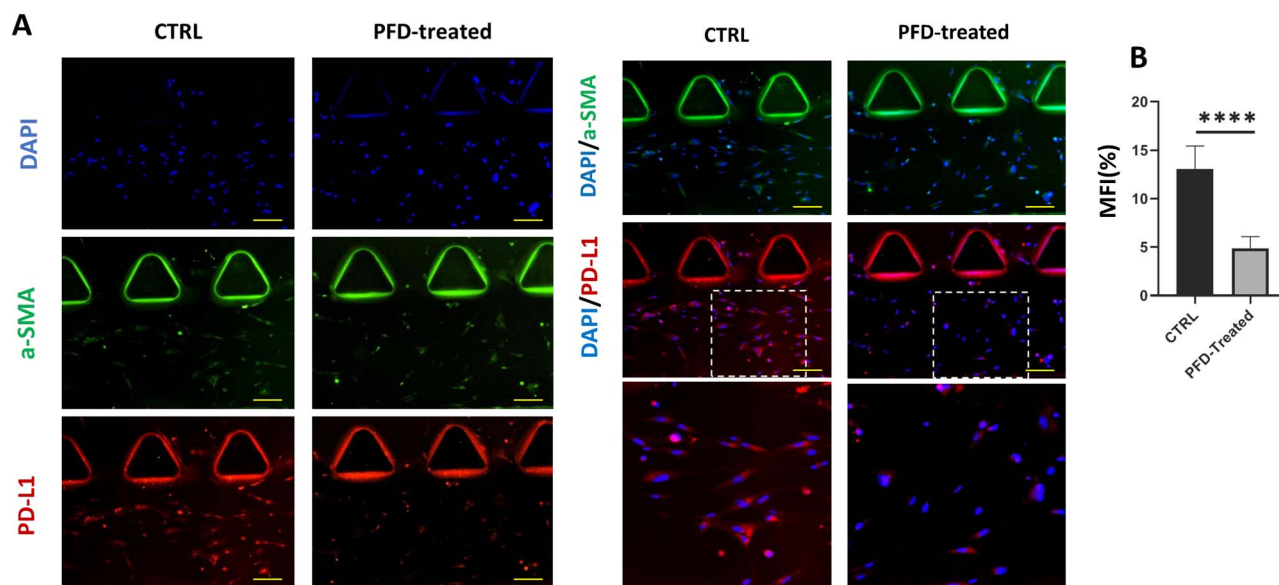

Figure 8. Effects of PFD on expression of PD-L1 in CAFs. (A) Immunofluorescent image of CAFs cultured and treated with or without PFD in microfluidic device and stained with α-SMA (green), PD-L1 (red) and nucleus (blue) (scale bar: 200 μm). (B) Quantification of MFI of PD-L1 expression in both un-treated and treated CAFs with PFD (n = 3) (P < 0.005).

targeting of IL6 and PD-L1 not only improves the infiltration of IFNγ-producing CD4+ T cells in tumor tissues but also enhances the expression of T-cells attracting related chemokines in TME. Consistence with these results, we show that CAF-CM significantly increased immunosuppression capacity of breast carcinoma cells through the expression of PD-L1, in which cytokine profiling and PPI network analysis depicted a positive

association between the secretion of IL6, IL8, CCL17 and CXCL1 with PD-L1. In addition to these data and line with previous studies [44], we also show that CAFs able to stimulate phenotype switch in carcinoma cells from a non-invasive to an invasive phenotype in which increased expression of vimentin in non-invasive carcinoma cells by CAFs can trigger EMT program and invasiveness. Additionally, we demonstrated that treatment
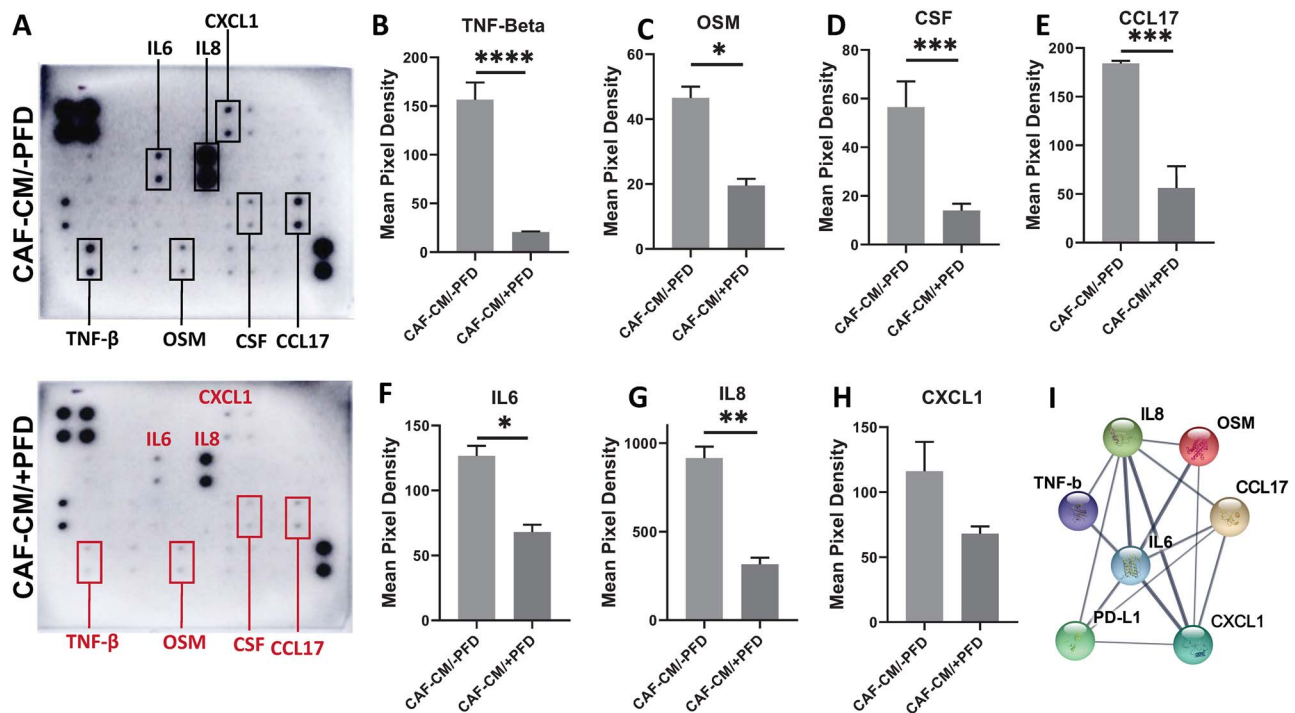
Figure 9. Cytokine profiling of CAF-CM. (A) The picture of cytokine array results performed for CAF-CM before and after treatment with PFD. The top left and bottom right dots are negative and positive control of array, respectively. (B–H) The mean pixel density analysis results of differentially released cytokines TNF-β (B) ($P < 0.005$), OSM (C), CSF (D), CCL17 (E), IL6 (F), IL8 (G) and CXCL1 (H) from CAF treated with (CAF-CM/+PFD) and without (CAF-CM/-PFD) PFD ($n = 3$). (I). Protein–protein interaction network and correlation analysis between differentially released cytokines and PD-L1.

CAFs cells with PFD decreased the migration potential of both CAFs and breast carcinoma cells modeled in a microfluidic device. Similar observations were reported previously for migratory inhibition effect of PFD on both cancer cells and CAFs in pancreatic cancer [18] and BC [45]. For instance, Ren and colleagues demonstrated that CAF-CM significantly induces the expression of HOTAIR and consequently promotes EMT program in invasive BC in which targeting CAFs with PFD blocks TGF-β1/HOTAIR axis and decreases the migration potential of MDA-MB-231 cells [45].

Taken together, at an *in vitro* stage, these data suggest that targeting CAFs with PFD may reduce both metastasis and immune suppressive capacity of CAFs in TME. Additionally, the potential application of PFD to deplete the secretion of the various cancer-promoting cytokines and chemokines expressed in different sub-types of BC (Fig. 2C) (Fig. 9) suggesting the potential of applying PFD in combination with current treatment regimens particularly immunotherapy. Further studies focused on complex models of TME, including genetically engineered mouse model included with immune systems elements, are required to approve the potential application of PFD on improving immunotherapy and chemotherapy efficacy.

SUPPLEMENTARY DATA

Supplementary data is available at *INTBIO Journal* online.

FUNDING

CONFLICT OF INTEREST STATEMENT

The authors reported no potential conflict of interest.

REFERENCES

1. Denkert C, Liedtke C, Tutt A *et al* Molecular alterations in triple-negative breast cancer—The road to new treatment strategies. *Lancet* 2017;**389**:2430–42.
2. Gascard P, Tlsty TD. Carcinoma-associated fibroblasts: Orchestrating the composition of malignancy. *Genes Dev* 2016;**30**:1002–19.
3. Wang L, Saci A, Szabo PM *et al* EMT- and stroma-related gene expression and resistance to PD-1 blockade in urothelial cancer. *Nat Commun* 2018;**9**:3503.
4. Khoo BL, Chaudhuri PK, Ramalingam N *et al* Single-cell profiling approaches to probing tumor heterogeneity. *Int J Cancer* 2016;**139**:243–55.
5. Costa A, Kieffer Y, Scholer-Dahirel A *et al* Fibroblast heterogeneity and immunosuppressive environment in human breast cancer. *Cancer Cell* 2018;**33**:463–79.e10.
6. Wen S, Hou Y, Fu L *et al* Cancer-associated fibroblast (CAF)-derived IL32 promotes breast cancer cell invasion and metastasis via integrin β3–p38 MAPK signalling. *Cancer Lett* 2019;**442**:320–32.
7. Benyahia Z, Dussault N, Cayol M *et al* Stromal fibroblasts present in breast carcinomas promote tumor growth and angiogenesis through adrenomedullin secretion. *Oncotarget* 2017;**8**:15744–62.
8. Orimo A, Gupta PB, Sgroi DC *et al* Stromal fibroblasts present in invasive human breast carcinomas promote tumor growth and angiogenesis through elevated SDF-1/CXCL12 secretion. *Cell* 2005;**121**:335–48.

9. Farmer P, Bonnefoi H, Anderle P *et al* A stroma-related gene signature predicts resistance to neoadjuvant chemotherapy in breast cancer. *Nat Med* 2009;**15**:68–74.

10. Wu X, Tao P, Zhou Q *et al* IL-6 secreted by cancer-associated fibroblasts promotes epithelial-mesenchymal transition and metastasis of gastric cancer via JAK2/STAT3 signaling pathway. *Oncotarget* 2017;**8**:20741–50.

11. Kraman M, Bambrough PJ, Arnold JN *et al* Suppression of antitumor immunity by stromal cells expressing fibroblast activation protein-alpha. *Science* 2010;**330**:827–30.

12. Kalluri R. The biology and function of fibroblasts in cancer. *Nat Rev Cancer* 2016;**16**:582–98.

13. Özdemir BC, Pentcheva-Hoang T, Carstens JL *et al* Depletion of carcinoma-associated fibroblasts and fibrosis induces immunosuppression and accelerates pancreas cancer with reduced survival. *Cancer Cell* 2014;**25**:719–34.

14. Takeda Y, Tsujino K, Kijima T *et al* Efficacy and safety of pirfenidone for idiopathic pulmonary fibrosis. *Patient Prefer Adherence* 2014;**361**.

15. Polydorou C, Mpekris F, Papageorgis P *et al* Pirfenidone normalizes the tumor microenvironment to improve chemotherapy. *Oncotarget* 2017;**8**:24506–17.

16. Takai K, Le A, Weaver VM *et al* Targeting the cancer-associated fibroblasts as a treatment in triple-negative breast cancer. *Oncotarget* 2016;**7**:3–6.

17. Brooks D, Zimmer A, Wakefield L *et al* Limited fibrosis accompanies triple-negative breast cancer metastasis in multiple model systems and is not a preventive target. *Oncotarget* 2018;**9**:23462–81.

18. Kozono S, Ohuchida K, Eguchi D *et al* Pirfenidone inhibits pancreatic cancer desmoplasia by regulating stellate cells. *Cancer Res* 2013;**73**:2345–56.

19. Binnewies M, Roberts EW, Kersten K *et al* Understanding the tumor immune microenvironment (TIME) for effective therapy. *Nat Med* 2018;**24**:541–50.

20. Yoshihara K, Shahmoradgoli M, Martínez E *et al* Inferring tumour purity and stromal and immune cell admixture from expression data. *Nat Commun* 2013;**4**:2612.

21. Chen X, Song E. Turning foes to friends: Targeting cancer-associated fibroblasts. *Nat Rev Drug Discov* 2019;**18**:99–115.

22. Azadi S, Aboulkheyr Es H, Razavi Bazaz S *et al* Upregulation of PD-L1 expression in breast cancer cells through the formation of 3D multicellular cancer aggregates under different chemical and mechanical conditions. *Biochim Biophys Acta, Mol Cell Res* 2019;**1866**:118526.

23. Sherman MH, Yu RT, Engle DD *et al* Vitamin D receptor-mediated stromal reprogramming suppresses pancreatitis and enhances pancreatic cancer therapy. *Cell* 2014;**159**:80–93.

24. Li C, Rezov V, Joensuu E *et al* Pirfenidone decreases mesothelioma cell proliferation and migration via inhibition of ERK and AKT and regulates mesothelioma tumor microenvironment in vivo. *Sci Rep* 2018;**8**:10070.

25. Sahai E, Astsaturov I, Cukierman E *et al* A framework for advancing our understanding of cancer-associated fibroblasts. *Nat Rev Cancer* 2020;**20**:174–86.

26. Liu T, Han C, Wang S *et al* Cancer-associated fibroblasts: An emerging target of anti-cancer immunotherapy. *J Hematol Oncol* 2019;**12**:86.

27. Kulasinghe A, Schmidt H, Perry C *et al* A collective route to head and neck cancer metastasis. *Sci Rep* 2018;**8**:746.

28. Kulasinghe A, Wu H, Punyadeera C *et al* The use of microfluidic technology for cancer applications and liquid biopsy. *Micromachines* 2018;**9**:397.

29. Chaudhuri PK, Ebrahimi Warkiani M, Jing T *et al* Microfluidics for research and applications in oncology. *Analyst* 2016;504–24.

30. Lambrechts D, Wauters E, Boeckx B *et al* Phenotype molding of stromal cells in the lung tumor microenvironment. *Nat Med* 2018;**24**:1277–89.

31. De Jaeghere EA, Denys HG, De Wever O. Fibroblasts fuel immune escape in the tumor microenvironment. *Trends Cancer* 2019;**5**:704–23.

32. Lakins MA, Ghorani E, Munir H *et al* Cancer-associated fibroblasts induce antigen-specific deletion of CD8 + T cells to protect tumour cells. *Nat Commun* 2018;**9**:948.

33. Fernández-Nogueira P, Mancino M, Fuster G *et al* Tumor-associated fibroblasts promote HER2-targeted therapy resistance through FGFR2 activation. *Clin Cancer Res* 2020;**26**:1432–48.

34. Biffi G, Oni TE, Spielman B *et al* IL1-induced JAK/STAT signaling is antagonized by TGFβ to shape CAF heterogeneity in pancreatic ductal adenocarcinoma. *Cancer Discov* 2019;**9**:282–301.

35. Casagrande N, Borghese C, Visser L, *et al* CCR5 antagonism by maraviroc inhibits Hodgkin lymphoma microenvironment interactions and xenograft growth. *Haematologica* 2019; **104**:564–75.

36. Highfill SL, Cui Y, Giles AJ *et al* Disruption of CXCR2-mediated MDSC tumor trafficking enhances anti-PD1 efficacy. *Sci Transl Med* 2014;**6**:237ra67.

37. Fares CM, Van Allen EM, Drake CG *et al* Mechanisms of resistance to immune checkpoint blockade: Why does checkpoint inhibitor immunotherapy not work for all patients? *Am Soc Clin Oncol Educ B* 2019;**39**:147–64.

38. Mizukami Y, Kono K, Kawaguchi Y *et al* CCL17 and CCL22 chemokines within tumor microenvironment are related to accumulation of Foxp3+ regulatory T cells in gastric cancer. *Int J Cancer* 2008;**122**:2286–93.

39. Gil M, Komorowski MP, Seshadri M *et al* CXCL12/CXCR4 blockade by Oncolytic Virotherapy inhibits ovarian cancer growth by decreasing immunosuppression and targeting cancer-initiating cells. *J Immunol* 2014;**193**:5327–37.

40. Omland SH, Wettergren EE, Mollerup S *et al* Cancer associated fibroblasts (CAFs) are activated in cutaneous basal cell carcinoma and in the peritumoural skin. *BMC Cancer* 2017;**17**:675.

41. Tsukamoto H, Fujieda K, Miyashita A *et al* Combined blockade of IL6 and PD-1/PD-L1 signaling abrogates mutual regulation of their immunosuppressive effects in the tumor microenvironment. *Cancer Res* 2018;**78**:5011–22.

42. Lamano JB, Lamano JB, Li YD *et al* Glioblastoma-derived IL6 induces immunosuppressive peripheral myeloid cell PD-L1 and promotes tumor growth. *Clin Cancer Res* 2019;**25**:3643–57.

43. Chan L-C, Li C-W, Xia W *et al* IL-6/JAK1 pathway drives PD-L1 Y112 phosphorylation to promote cancer immune evasion. *J Clin Invest* 2019;**129**:3324–38.

44. Truong DD, Kratz A, Park JG *et al* A human organotypic microfluidic tumor model permits investigation of the interplay between patient-derived fibroblasts and breast cancer cells. *Cancer Res* 2019;**79**:3139–51.

45. Ren Y, Jia H, Xu Y *et al* Paracrine and epigenetic control of CAF-induced metastasis: The role of HOTAIR stimulated by TGF-ß1 secretion. *Mol Cancer* 2018;**17**:5.